

Simultaneous Reconstruction of Image and Motion in Gated Positron-Emission-Tomography

Moritz Blume, Andreas Keil, Axel Martinez-Moeller, Nassir Navab, Magdalena Rafecas

Abstract—We present a novel method for joint reconstruction of both image and motion in positron-emission-tomography (PET). Most of nowadays motion compensation methods consist of two completely separated steps: (i) motion estimation and (ii) image estimation. A major drawback of these methods lies in the motion estimation step, since it is completely based on the usually noisy individually reconstructed gates. As we show in a simulation study, a joint reconstruction approach alleviates this drawback and results in both visually and quantitatively better image quality. We attribute these results to the fact that for motion estimation always the currently best available image estimate is used and vice versa. Additionally, results for dual respiratory and cardiac gated patient data are presented.

I. INTRODUCTION

Most of nowadays motion compensation methods for PET consist of two steps: they first estimate the motion, and then, based on this motion estimate, they estimate the image (refer to [1]–[3], just to name a few). The first step is usually accomplished by an image registration/optical flow technique, applied to the individually reconstructed gates. The second step can be done by transforming these individually reconstructed gates according to the previously gathered motion and then taking the sum. It is also possible to perform a 4D ML-EM reconstruction based on the motion estimate, such as proposed in [4].

A major problem of methods that separate motion estimation from image estimation is, that the motion estimate is becoming more and more inaccurate with increasing noise. In order to overcome these problems, joint estimation methods that maximize a 4D likelihood expression have been proposed [5], [6].

Our approach is based on a very similar objective function as [6], however, our optimization scheme is different. In contrast to [6], we observe a clear advantage for joint reconstruction methods with respect to reconstruction quality. [5] uses a different cost function that incorporates several image estimates, while our cost function is based on just one image estimate.

M. Blume and M. Rafecas are with the Instituto de Física Corpuscular (IFIC), Universidad de Valencia / CSIC, Valencia, Spain. M. Blume, A. Keil and N. Navab are with the research group Computer Aided Medical Procedures (CAMP), Department of Computer Science, Technische Universität München, Munich, Germany. A. Martinez-Moeller is with the Nuklearmedizinische Klinik, Technische Universität München, Munich, Germany. Author contact: Moritz Blume, IFIC - Instituto de Física Corpuscular, Edificio Institutos de Investigación, Apartado de Correos 22085, E-46071 Valencia - Spain, Phone: +34963543237, E-Mail: moritz.blume@cs.tum.edu. This work was supported by the Spanish Ministry of Education and Science (Grant TEC2007-61047).

II. METHODS

A. Joint Reconstruction

In the following, we develop a cost functional

$$\mathcal{J}(f, \varphi) = \mathcal{D}(f, \varphi) + \alpha \mathcal{S}(\varphi) \quad (1)$$

which depends on both image f and motion φ and is subject to minimization.

1) *Dissimilarity Term*: The number of counts $g(a, t)$ that is measured for a line-of-response (LOR) a in gate t underlies a Poisson distribution:

$$P(g(a, t)|f, \varphi) = e^{-\hat{g}(a, t)} \cdot \frac{\hat{g}(a, t)^{g(a, t)}}{g(a, t)!} \quad (2)$$

f is the image function and $\varphi(\mathbf{x}, t)$ represents the deformation field at gate t with respect to a virtual reconstruction frame.

$$\hat{g}(a, t, f, \varphi) = \frac{1}{T} \int H(a, \mathbf{x}) f(\varphi(\mathbf{x}, t)) d\mathbf{x} \quad (3)$$

is the expected measurement vector. $H(a, \mathbf{x})$ is the system model which contains the probability that the two annihilation photons emitted at position \mathbf{x} will be measured in LOR a .

The likelihood function for all measured events of a gate t is

$$L(f, \varphi|g(a, t)) = \prod_a P(g(a, t)|f, \varphi) \quad (4)$$

We seek to find a pair of image f and motion φ that maximizes the likelihood function for all gates. This maximization is equivalent to minimizing $-\log(L(f, \varphi))$, and we finally arrive at

$$\mathcal{D}(f, \varphi) = \sum_{t, a} \hat{g}(a, t, f, \varphi) - g(a, t) \log(\hat{g}(a, t, f, \varphi)) \quad (5)$$

(the term $\sum_{t, a} \log(g(a, t)!)$ was omitted since it does not affect the minimum).

2) *Regularization*: In order to prohibit extreme deformations we use a homogeneous diffusion regularization term

$$\mathcal{S}(\varphi) = \sum_t \sum_{i=1}^3 \int \|\nabla_{\mathbf{x}} \varphi_i(\mathbf{x}, t)\|^2 d\mathbf{x} \quad (6)$$

which is well known in the image registration community. The regularization parameter α defines the smoothness of our sought deformation function.

B. Optimization

We optimize \mathcal{J} by calculating the variational gradients with respect to f and φ and performing an alternating update scheme.

C. Evaluation

We test our algorithm for both simulated and real data.

1) *Simulation*: We generate 32 frames using the XCAT phantom [7]. One complete respiratory cycle of a length of five seconds is simulated, without any cardiac motion. The extent of diaphragm motion is set to two centimeters. These 32 frames are then redistributed to eight gates. In doing so we make sure that motion is simulated also within a gate. For each gate, a volume of $50 \times 50 \times 50$ voxels containing the heart is cropped.

The expected number of counts for each LOR is calculated by projecting each gate to measurement space. The measurements are finally generated from the expected number of counts by a Poisson random generator. This way we take into account the acquisition time and activity. Ten levels of statistical noise, representing very long to extremely short acquisition times, were simulated.

Since we want to focus on image degradations induced by motion, we did not make use of external simulation packages which would include effects like scattering, random coincidences etc. We simulate a Siemens Biograph Sensation 16 PET/CT scanner and use Scheins's algorithm to generate the system matrix [8].

2) *Real Data*: The patient data was taken from a previously accomplished cardiac examination which measured the myocardial metabolism in order to assess tissue viability. It was acquired with a Siemens Biograph Sensation 16 PET/CT scanner. The injected dose of ^{18}F -FDG was roughly 400 MBq. The patient had to rest for 60 minutes before data acquisition started. Both the respiratory and the ECG signal were recorded and later used in order to divide the data into eight respiratory gates by omitting the systolic phase and combining all diastolic phases into one (since the diastolic phase is the longest cardiac phase with minimal motion). As for the simulation, we also use Scheins's algorithm for calculating the system matrix.

3) *Registration and Fusion of Reconstructed Frames (RFRF)*: For comparison, we implemented two ambassadors of RFRF methods which only differ in the image estimation part.

a) *Motion Estimation*: Motion estimation consists of individual reconstruction of each gate and its registration to a reference gate (in our case the first gate). The registration is done by minimizing the squared difference between the reference and the template image. Homogeneous diffusion regularization is applied to the motion function in order to encourage physically meaningful solutions.

b) *Image Estimation*: The first image estimation method (RFRF 1) consists of a summation of the transformed gates, similar as in [3]. In the second method (RFRF 2), the image is completely re-reconstructed based on the whole data (refer to [9], [10] for details).

4) *Comparison*: For the simulated data, we compare our joint reconstruction approach (JR) to an ML-EM reconstruction (30 iterations) for motion-contaminated data (MC), an ML-EM reconstruction (30 iterations) for the first gate (FG), the two RFRF approaches and an ML-EM reconstruction (30 iterations) for motion-free data (MF).

As a quantitative measure for evaluation we use the correlation coefficient $\mathcal{CC}(\mathbf{x}, \mathbf{y}) = \frac{\mathbf{x}^T \mathbf{y}}{\|\mathbf{x}\| \|\mathbf{y}\|}$ between the reconstructed image of the respective reconstruction approach (represented by a vector \mathbf{x}) and the original image (represented by a vector \mathbf{y}). Both \mathbf{x} and \mathbf{y} are shifted such that their mean value is zero.

For real data, JR is compared to MC, FG and RFRF 1. Note that since no ground truth data is available, no quantitative comparison could be performed.

III. RESULTS AND DISCUSSION

A. Simulation

Table I summarizes the results for different noise levels. Figure 2 shows visually selected transverse, coronal and sagittal slices for three levels of noise. The level of noise is indicated by the number of annihilation events - the less events, the higher the level of noise.

JR performs better or equal than MC, FG and RFRF in all cases. Especially for moderate and high noise levels the difference is striking.

Comparing JR to MF, it is surprising that JR has an even higher correlation coefficient for high noise levels. Consulting Figure 2c reveals that this observation may be attributed to the fact that the joint reconstruction is less noisy than the reconstruction for motion-free data.

Interestingly, RFRF 1 works better than MC only for low and moderate noise levels. An explanation may be that fusion by summation *in image space* is a permissible approximation only for low-noise scenarios. Also, we expected RFRF 2 to perform better than RFRF 1 not only for low levels of noise. It seems that RFRF 2 is very sensitive to the previously estimated motion function.

B. Real Data

Figure 1 compares our joint reconstruction approach (fourth column) to MF, FG and RFRF 1. It clearly shows the better defined myocardial walls, indicating the potential of our method to achieve a notable reduction of the motion induced blur.

REFERENCES

- [1] G. J. Klein, B. W. Reutter, and R. H. Huesman, "Non-rigid summing of gated PET via optical flow," in *Nuclear Science Symposium, 1996. Conference Record., 1996 IEEE*, vol. 2, Anaheim, CA, USA, Nov. 1996, pp. 1339–1342.
- [2] —, "4d affine registration models for respiratory-gated PET," in *Nuclear Science Symposium Conference Record, 2000 IEEE*, vol. 2, Lyon, France, 2000, pp. 41–15.
- [3] M. Dawood, N. Lang, X. Jiang, and K. P. Schäfers, "Lung motion correction on respiratory gated 3-D PET/CT images," *IEEE Transactions on Medical Imaging*, vol. 25, no. 4, pp. 476–485, Apr. 2006.
- [4] F. Qiao, J. W. Clark, T. Pan, and O. Mawlawi, "Expectation maximization reconstruction of PET image with non-rigid motion compensation," in *Engineering in Medicine and Biology Society, 2005. IEEE-EMBS 2005. 27th Annual International Conference of the*, Sep. 2005, pp. 4453–4456.

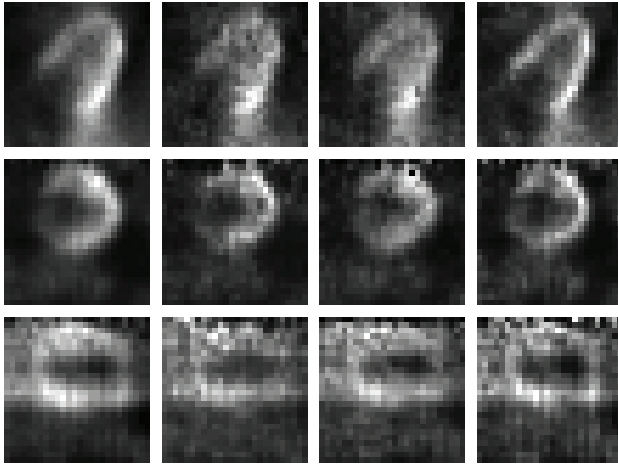
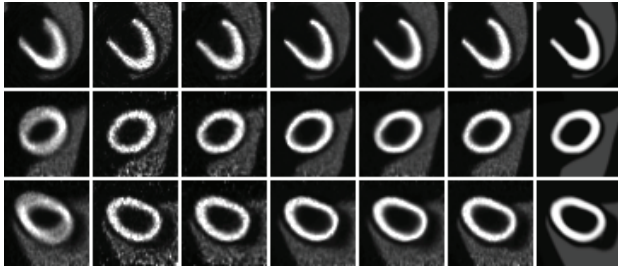
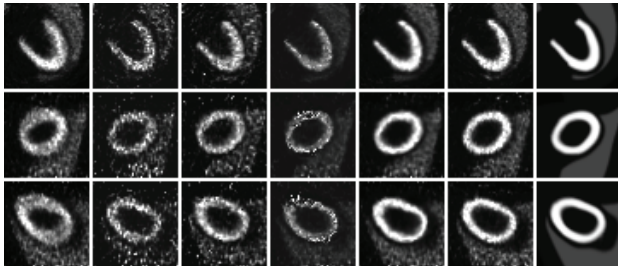


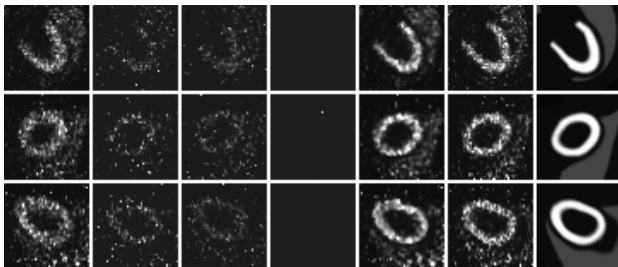
Fig. 1: Transverse, coronal and sagittal slices for real patient data (from left to right): MC, FG, RFRF 1 and JR.



(a) Moderate noise: 4.50×10^7 annihilation events



(b) High noise: 5.60×10^6 annihilation events



(c) Extremely high noise: 7.00×10^5 annihilation events

Fig. 2: Selected transverse, coronal and sagittal slices for different levels of noise and different reconstruction scenarios for the simulated data (from left to right): MC, FG, RFRF 1, RFRF 2, JR and MF. For comparison, the original image is shown in the last column.

Counts	MC	FG	RFRF 1	RFRF 2	JR	MF
3.60×10^8	0.93	0.99	0.98	0.99	0.99	0.99
1.80×10^8	0.93	0.98	0.98	0.99	0.99	0.99
9.00×10^7	0.93	0.97	0.98	0.98	0.98	0.99
4.50×10^7	0.93	0.95	0.96	0.98	0.98	0.99
2.25×10^7	0.92	0.91	0.93	0.96	0.98	0.98
1.13×10^7	0.91	0.85	0.90	0.91	0.97	0.97
5.60×10^6	0.88	0.74	0.81	0.67	0.96	0.95
2.80×10^6	0.84	0.62	0.60	0.28	0.93	0.91
1.40×10^6	0.76	0.48	0.45	0.0078	0.87	0.85
7.00×10^5	0.65	0.36	0.33	0.016	0.78	0.74

TABLE I: Simulation: quantitative evaluation for different reconstruction scenarios.

- [5] B. A. Mair, D. R. Gilland, and Z. Cao, "Simultaneous motion estimation and image reconstruction from gated data," in *Biomedical Imaging, 2002. Proceedings. 2002 IEEE International Symposium on*, 2002, pp. 661–664.
- [6] M. Jacobson and J. Fessler, "Joint estimation of image and deformation parameters in motion-corrected pet," in *Nuclear Science Symposium Conference Record, 2003 IEEE*, vol. 5, 19-25 Oct. 2003, pp. 3290–3294Vol.5.
- [7] W. P. Segars, "Development and application of the new dynamic nurbs-based cardiac-torso (ncat) phantom," Ph.D. dissertation, University of North Carolina, 2001.
- [8] J. J. Scheins, F. Boschen, and H. Herzog, "Analytical calculation of volumes-of-intersection for iterative, fully 3-d PET reconstruction," *IEEE Transactions on Medical Imaging*, vol. 25, no. 10, pp. 1363–1369, Oct. 2006.
- [9] F. Qiao, T. Pan, J. W. C. Jr, and O. R. Mawlawi, "A motion-incorporated reconstruction method for gated pet studies," *Physics in Medicine and Biology*, vol. 51, no. 15, pp. 3769–3783, 2006. [Online]. Available: <http://stacks.iop.org/0031-9155/51/3769>
- [10] F. Lamare, M. J. L. Carbayo, T. Cresson, G. Kontaxakis, A. Santos, C. Cheze, L. Rest, A. J. Reader, and D. Visvikis, "List-mode-based reconstruction for respiratory motion correction in PET using non-rigid body transformations," *Physics in Medicine and Biology*, vol. 52, no. 17, pp. 5187–, 2007.